Incidence and properties of nanoscale defects in silicalite†

Naseem A. Ramsahye and Ben Slater*

Received (in Cambridge, UK) 26th September 2005, Accepted 4th November 2005
First published as an Advance Article on the web 8th December 2005
DOI: 10.1039/b513582f

Crystal intergrowths are predicted to form more readily than other extended defects in a model zeolite membrane and cause a reduction in molecular flux.

Silicalite (hereafter referred to by its framework code, MFI) is widely used in the petrochemical industry for separating light fractions of oil and upon doping with titanium, it acts as an important catalyst in the preparation of epoxides. Key to efficient sieving is the preparation of regular, obstruction free channels that are often deployed as thin oriented sheets or membranes. Zeolite materials, often termed inorganic polymers, are composed of aluminosilicate frameworks, built from corner sharing TO_4 (T = Si/Al) tetrahedra. This class of materials typically form continuous and uninterrupted networks of bonds, although some zeolites do not conform to this definition, such as cloverite.[1] When interruptions occur, the undercoordinated T or oxygen sites are assumed to protonate because of the presence of water during synthesis. Dissociative adsorption of water and/or the readily available hydroxyl species gives rise to silanol species thus enhancing the intrinsic acidity of the solid. Whilst acidity is generally advantageous to catalysis, it degrades the thermal stability of the material and consequently its longevity. In addition, the presence of crystal defects may help or hinder transport of reagents/products from the catalytically active site. Interruptions can occur due to misregistrations in the layer-by-layer crystal growth assembly process, leading to unusual apertures within the framework[2] that transgress into the mesoscale. In MFI, to optimise the efficacy of membranes, it is therefore important to understand what defects can occur and to understand their potential benefit or deficit to sieving capability.

MFI is composed of pentasil chains (highlighted in Fig. 1b) that can be connected in many permutations, giving rise to other materials, such as the closely related framework MEL.[3] These chains are in fact chiral and can be registered with respect to each other in many ways. The reader is referred to a discussion on MFI/MEL crystal relations for clarification.[4] In previous work, Ohsuna *et al.*[4] and Millward *et al.*[5] have identified two types of extended defects within MFI. The focus of this work is to assess the energetic cost of typical defects (to infer their relative populations) and how they change the transport properties of the material.

In total we have examined three types of interruption defects, two of which have been observed in MFI. In Fig. 1, a composite shows the perfect zeolite structure with the defect observed by

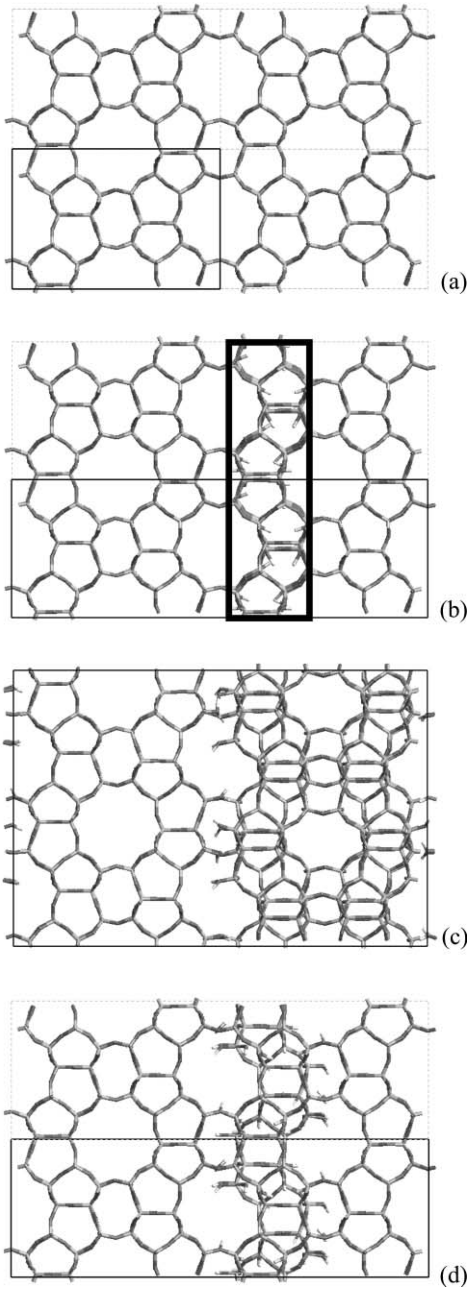

Fig. 1 Figures a–d show the view along the [010] plane through the unit cell (replicated for clarity). Views along the [001] axis are shown in the supporting information. Silicon atoms are shown in dark grey, oxygen atoms depicted in mid-grey and hydrogen is shown in white. (a) is the perfect MFI lattice, (b) is the O defect, (c) is the M defect and (d) is the R defect (see text for description).

Davy Faraday Research Laboratory, The Royal Institution of Great Britain, 21 Albemarle Street, London, UK W1S 4BS.
E-mail: ben@ri.ac.uk; Fax: +44 207 629 3569; Tel: +44 207 670 2955
† Electronic supplementary information (ESI) available: XYZ coordinates of the relaxed structures are included for visualisation purposes. See DOI: 10.1039/b513582f

Ohsuna and Terasaki (O), that proposed by Millward *et al.* (M) and a hypothetical defect (R). The O linear defect arises when one of the pentasil chains is rotated by 90° and translated by *b*/2 along the *b* axis, giving a partially interrupted structure where half the Si/O bonds are in registry with the matrix of bonds and half are undercoordinated. The M defect is formed when multiple crystal layers grow at 90° with respect to the substrate (a rotational intergrowth). This defect gives rise to interruptions at the interface. The R defect is formed by rotating a single pentasil chain by 90°, about the *b* axis. This defect gives rise to a fully interrupted structure, and the defect is notionally held in place by hydrogen bonding.

Using interatomic potential methods, based on the Born model of solids, we relaxed the defects within the crystal (GULP[6]). Interatomic potentials originate from Sanders *et al.*[7] and have been shown to give both accurate energies and structures and have an established pedigree. We calculate that the costs of introducing the defects into the crystal, expressed as stacking fault energies, are 184 mJ m^{-2}, 419 mJ m^{-2} and 613 mJ m^{-2} for the O, M and R defects respectively, accounting for dissociative adsorption of water at undercoordinated sites using a scheme proposed by Parker *et al.*[8] In their approach, the material dependent, second electron affinity energy for the oxygen atom is computed *via* a Born–Haber scheme, which also includes a correction for the formation of gaseous water from the liquid state. The gaseous water is then computationally dissociated into OH^- and H^+ fragments that are attached to undercoordinated silicon and oxygen sites respectively. For comparison, we also calculated the energy of forming a regular stacking fault between MFI and MEL, which gives rise to a continuous structure. This class of defect is readily observed in crystal samples[4,9] and has been discussed in some detail by Thomas and Millward. By comparison, the stacking fault energy is just 27 mJ m^{-2}, clearly suggesting that such a defect could be formed more readily than the interrupted structures we have studied. Note that although the stacking fault energies are considerably larger than those found for metals, they are somewhat smaller than stacking faults computed using first-principles for a silicate mineral forsterite,[10] which has a lower compressibility than a zeolitic material, suggesting the energies reported here are reasonable. There is another important defect in MFI—the twin, which is very commonly observed. In contrast to the 90° overgrowth seen in the M defect, the intersection between the faces is at a more acute angle. For further details and discussion, the reader is referred to Agger *et al.*[11] but these defects are not considered here.

Comparing defect energies, which we take to be indicative of the relative defect populations, we can conclude that the MFI/MEL defect is most likely to be observed followed by the O, M and R defects respectively. Note that although the R defect is most unfavourable, the energy cost per unit length is comparable to the cost of introducing a dislocation into zeolite A, which has been observed in zeolite A crystals.[12] Therefore, it is reasonable to suppose that all of these defects may be present in MFI crystallites, albeit in very different concentrations and their presence could affect molecular transport.

MFI contains two channel systems, a straight channel running along [010] and a sinusoidal parallel to [100]. For membrane applications, MFI is normally grown oriented with respect to the *b* axis because the straight channel permits greater molecular flux than the more tortuous channel. A test probe in the form of a carbon dioxide molecule was used to gauge whether silanol groups pose a significant obstacle to the minimum energy pathway for diffusion. Recently Jaramillo and Chandross[13] have published studies of CO_2 adsorption in LTA, which were carefully fitted to reproduce the experimentally measured isotherms. We have slightly modified this potential to reproduce the enthalpy of adsorption and barrier heights for the fully ionic model of the host used here. In this work, the defects have been aligned within the [010] channel, but because of the interconnectivity between channel systems, the planar defects will impact on transport in both [010] and [100] channel systems. The probe is incrementally positioned through the crystal (adjacent to the plane defect), using a constrained optimisation procedure that we have used previously to explore external surface migration.[14] At each stage, the energy is recorded and a potential energy landscape is built up which defines the maximum barrier to diffusion with respect to a given axis and channel system. In Table 1, the barrier heights for diffusion in the perfect and defective materials are recorded.

The M and R defects cause a large increase in the barrier height which is greater than the barrier height in the [100] direction of the perfect material. Diffusion in the proximity of the O defect is substantially smaller than other defects but it is found to be much greater than the barrier height associated with the MFI/MEL intergrowth in the [010] direction. Unsurprisingly, all the defects cause an increase in the barrier height in the [100] direction relative to the perfect material, which suggests that the fastest process measured by NMR (for example) will be that parallel to [010] and slower diffusion processes will occur along the [100] channel. It should be noted that 1D diffusion has been simulated, to estimate the barrier height along a given channel. The [100] and [010] channel systems are interconnected and hence at moderate temperatures, 3D diffusion of CO_2 may occur *via* the intersection between channels (in the perfect lattice). When more bulky guests are present within the lattice, single-file diffusion occurs at lower temperatures, which would be rate-limited by the presence of each defect considered here.

By inference, defect formation in the [100] direction would be expected to increase barrier heights in [010] substantially because of the connectivity between the pentasil chains. By contrast, diffusion along [010] in the MFI/MEL intergrowth is comparable with the perfect material. Note that the intergrowth we have considered contains a half cell of MEL, which means that the most tortuous part of the MEL pathway is reduced relative to the pure MEL material, explaining why the intergrowth pathway is more favourable than the MEL pathway. The M, O and R defects exhibit silanol groups that protrude into the channels that provide the largest barriers to transport and hence their effect on single-file transport along these channels will be dramatic.

Table 1 Barrier heights in perfect and defective MFI

Material	Barrier in [010]/eV	Barrier in [100]/eV
Perfect MFI	0.048	0.242
M	0.315	0.302
O	0.199	0.331
R	0.479	Impassable
MFI/MEL	0.069	0.346
Perfect MEL	0.173	0.173

A long standing source of controversy in the literature is the disparity of diffusion rates measured by different experimental techniques (see Karger and Ruthven[15] for example) that probe different time and lengthscales. Recent PFG NMR work that probes the microscopic lengthscale has provided seemingly clear evidence for the presence of intracrystalline defects within MFI.[16] Consideration of both the relative energies of each type of defect, coupled with their effects on diffusion barrier heights leads to the conclusion that intracrystalline barriers are expected to be due to MFI/MEL intergrowths rather than interruption defects. Although interruption defects are inferred to cause a huge reduction in molecular flux, their incidence is predicted to be very low in comparison to intergrowth populations (assuming template-free conditions). Furthermore, the O and R defects are linear, rather than planar and hence their perturbation upon diffusion pathways will be somewhat localised in contrast to planar defects.

In these calculations, the role of the template is not implicitly or explicitly modelled. Templates such as tetra-propyl ammonium (TPA) salts are typically used to synthesise MFI, which reduce the induction time to nucleation and enhance the crystallinity of the material. The structure directing properties of the TPA template cation favour the formation of MFI rather than MEL and hence one assumes, this disfavours the population of intergrowth defects. It can be supposed that the relative populations of each defect studied here will be sensitive to both the concentration and steric properties of the template used to synthesise MFI. The sticking probability of nuclei at the surface will be sensitive to the roughness of the surface, which will be influenced by the presence of templates and hence these kinetic factors may also control defect populations. Notwithstanding these comments, TPA can be easily hosted in MEL and hence the intergrowth is still expected to be the most prevalent defect in MFI.

Direct experimental measurement of defect incidence is difficult. HRTEM probably offers the most quantitative insight into defect density, but different slices through a large number of distinct crystal samples are needed, in order to obtain reliable statistics. Such an undertaking would be an extremely time intensive and laborious process but the advent of tomographic techniques may offer a means of obtaining defect statistics on a more tractable timescale.[16] In the absence of quantitative defect incidence data, since the intergrowth and O defect have been observed and strong evidence for the existence of the M defect has been presented, the absence of data confirming the existence of the R defect could be taken to be indicative of its rarity, which tallies with the prediction that this defect is the least favourable and populous of those we have considered.

In summary, the small but endothermic formation energy of intergrowths in MFI implies these defects may form in high concentrations and highlights the need to finely control crystal growth at the molecular level (through templates, inhibitors or other synthesis parameters), enabling the engineering of perfectly registered materials for optimal molecular sieving and transport.

Financial support from the EPSRC (GR/R81510) is gratefully acknowledged. The authors would like to thank the anonymous referees who made a number of useful suggestions.

Notes and references

1 M. Estermann, L. B. McCusker, Ch. Baerlocher, A. Merrouche and H. Kessler, *Nature (London)*, 1991, **352**, 320.
2 T. Ohsuna, B. Slater, F. Gao, J. Yu, Y. Sakamoto, G. Zhu, O. Terasaki, D. E. W. Vaughan, S. Qiu and C. R. A. Catlow, *Chem.–Eur. J.*, 2004, 5031.
3 G. T. Kokotailo, P. Chu, S. L. Lawton and W. M. Meir, *Nature (London)*, 1978, **255**, 119.
4 O. Terasaki, J. M. Thomas, G. R. Millward and D. Watanabe, *Chem. Mater.*, 1989, **1**, 158; J. M. Thomas and G. R. Millward, *J. Chem. Soc., Chem. Commun.*, 1982, 1380; T. Ohsuna, O. Terasaki, Y. Nakagawa, S. I. Zones and K. Higara, *J. Phys. Chem. B*, 1997, **101**, 9881.
5 G. R. Millward, S. Ramdas, J. M. Thomas and M. T. Bartlow, *J. Chem. Soc., Faraday Trans. 2*, 1983, **79**, 1075.
6 J. D. Gale and A. L. Rohl, *Mol. Simul.*, 2003, **29**, 291.
7 M. J. Sanders, M. Leslie and C. R. A. Catlow, *J. Chem. Soc., Chem. Commun.*, 1984, **19**, 1271.
8 S. C. Parker, N. H. de Leeuw and S. E. Redfern, *Faraday Discuss.*, 1999, **114**, 381.
9 G. González, W. Stracke, Z. Lopez, U. Keller, A. Ricker and R. Reichelt, *Microsc. Microanal.*, 2004, **10**, 224.
10 J. Durinck, A. Legris and P. Cordier, *Am. Mineral.*, 2005, **90**, 1072.
11 J. R. Agger, N. Hanif, C. S. Cundy, A. P. Wade, S. Dennison, P. A. Rawlinson and M. W. Anderson, *J. Am. Chem. Soc.*, 2003, **125**, 830–839.
12 S. Dumrul, S. Bazzana, J. Warzywoda, R. R. Biederman and A. Sacco Jr., *Microporous Mesoporous Mater.*, 2002, **54**, 79–88.
13 E. Jaramillo and M. Chandross, *J. Phys. Chem. B*, 2004, **108**, 20155.
14 L. Whitmore, B. Slater and C. R. A. Catlow, *Phys. Chem. Chem. Phys.*, 2000, **2**, 5354.
15 J. Karger and D. M. Ruthven, *Zeolites*, 1989, **9**, 267.
16 A. J. Koster, U. Ziese, A. J. Verkleij, A. H. Janssen and K. P. de Jong, *J. Phys. Chem. B*, 2000, **104**, 9368–9370.

